

# The study of bimolecular reactions under non-pseudo-first order conditions

Francesco Malatesta\*

*Department of Pure and Applied Biology, University of L'Aquila, L'Aquila, Italy*

Received 12 April 2005; received in revised form 25 April 2005; accepted 25 April 2005

Available online 17 May 2005

## Abstract

In this work a new equation which describes the time evolution of bimolecular reactions is derived and tested by experiment. The equation is general and the results show that second-order reactions of any simple type may be accurately described by a quotient of exponential functions. The model and reagent concentration dependent observed rate constants show a complex non-linear behaviour when experimental conditions deviate from pseudo-first order nevertheless reducing to the well-known linear dependence when pseudo-first order conditions are met.

© 2005 Elsevier B.V. All rights reserved.

**Keywords:** Bimolecular reactions; Binding; Pseudo-first order conditions; Electron transfer

## 1. Introduction

The study of bimolecular reactions is usually carried out under pseudo-first order (PFO) conditions by keeping the initial concentration of one of the two reagents in large excess (50–100 fold). This has the advantage of yielding a simple exponential time course, with the observed rate constant being directly related to the product of the initial concentration of the reagent in excess to the forward bimolecular rate constant. In the case of a simple reversible or irreversible bimolecular reaction, a plot of the observed rate constant *versus* the concentration of the reagent being varied will result in a linear relationship if pseudo-first order conditions are met. The slope of this plot yields the apparent bimolecular rate constant for the reaction, under the chosen experimental conditions.

Under non pseudo-first order conditions, i.e. when the initial concentrations of the reagents are comparable, the observed time course will deviate from a simple exponential

relaxation and typically the data may be fit to the sum of two or more exponential functions yielding an empirical description of the system. Thus, although bimolecular processes may be accounted for by a sum of exponential functions, the mathematical relationship of the fitted rate constants to the forward and reverse bimolecular rate constants is not straightforward and *de facto* hardens the physical description of the system under study. Here I show that the time course of a bimolecular reaction is described by a quotient of exponential relaxations and that considerable knowledge may be gained by studying bimolecular reactions under non-pseudo-first order conditions.

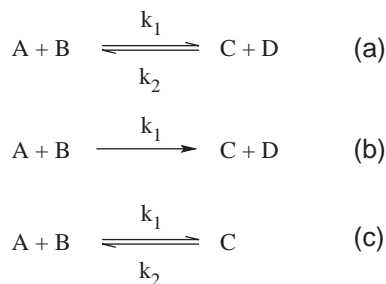
## 2. Materials and methods

Horse heart myoglobin, sodium ascorbate and potassium hexacyanoferrate III were purchased from Sigma-Aldrich. In CO combination experiments, 2 or 200  $\mu\text{M}$ , 1 mM dithionite-reduced myoglobin, in 0.1 M potassium phosphate pH 7.1, was mixed in the thermostated stopped-flow apparatus (Applied Photophysics) against a solution of CO of varying concentrations from 0.012 to 1 mM. 1-mM CO stock solutions were prepared in a tonometer at 20 °C by repeatedly degassing the buffer solution and applying a

*Abbreviations:* ET, electron transfer; PFO, pseudo-first order.

\* Dipartimento di Biologia di Base ed Applicata, Università di L'Aquila, Via Vetoio-Loc. Coppito, 67010 L'Aquila, Italy. Tel.: +39 0862433287; fax: +39 0862433273.

*E-mail address:* malatesta@univaq.it.



Scheme 1.

1-atm pressure from a CO tank to the tonometer. 1 mM sodium dithionite was thereafter added to the stock solution. Solutions of desired CO concentrations were prepared by anaerobic dilution of the stock CO solution to the desired concentration with buffer containing 1 mM sodium dithionite. Transients were recorded at 579.4 nm  $T=19.3$  °C.

The electron transfer reaction between sodium ascorbate and hexacyanoferrate III was followed at 420 nm at 20 °C in 5 mM potassium phosphate buffer pH 7.0.

The  $\text{Cu}_A$  and cytochrome  $c_{552}$  soluble domains from *Paracoccus denitrificans* were prepared as described previously [1,2] and were a kind gift of B. Ludwig and O. Maneg of J.W. Goethe-Universität, Frankfurt. The proteins were dissolved in  $\text{N}_2$ -flushed 20 mM Bis-Tris pH 7, containing 50 mM potassium chloride. In the forward (or reverse) electron transfer reaction 0.5 mM ascorbate was added to the cytochrome  $c_{552}$  (or  $\text{Cu}_A$ ) stopped-flow syringe to achieve complete reduction. Transients were recorded at 8 °C and at 551 nm as described previously [2]. All calculations and graphical procedures were performed using the Matlab or Micromath softwares. Initial values of the relevant parameters were first determined by using a simplex algorithm and thereafter used as entries for the Levenberg–Marquardt fitting algorithm.

### 3. Results and discussion

**Theory.** The most general elementary bimolecular reaction mechanisms are shown in Scheme 1.

Within the framework of the transition-state theory [3,4], the reagents approach by diffusion, form a precursor complex

stabilized by electrostatic and/or hydrophobic interactions, are pushed into the activated complex if sufficient collisional energy is available and eventually convert to products. The following analysis applies to all experimental situations whereby no precursor complex is stabilized along the reaction coordinate or may be isolated in vitro, otherwise stated whenever the collisional complex coincides with the transition state in which transfer of matter (electrons or atoms) within the partners is extremely facile. The solution of the rate equation which describes these mechanisms (detailed in the Supplementary Material for the mechanism in Scheme 1a, yet readily applicable to other mechanisms shown in Scheme 1) is the following expression:

$$x = x_{\text{EQ}} \frac{1 - e^{-\eta t}}{1 + \omega e^{-\eta t}} \quad (1)$$

Here,  $x$  represents the amount of reagents converted to products,  $x_{\text{EQ}}$  the equilibrium concentration change at infinite time,  $\eta$  the observed rate constant, and  $\omega$  a parameter (with values in the  $-1 < \omega < 1$  range) describing the deviation of the experimental setup from pseudo-first order conditions under the chosen experimental conditions. All parameters in Eq. (1) are functions of the forward and reverse (where applicable) bimolecular rate constants ( $k_1$  and  $k_2$ ) and of the initial reagent and product concentrations ( $A_0$ ,  $B_0$ ,  $C_0$  and  $D_0$ ):

$$\eta = \sqrt{\beta^2 - 4\alpha\gamma} \quad (2)$$

$$x_{\text{EQ}} = \frac{2\gamma}{\eta + \beta} \quad (3)$$

$$\omega = \frac{\eta - \beta}{\eta + \beta} \quad (4)$$

The model dependent constants  $\alpha$ ,  $\beta$  and  $\gamma$ , here referred to as primary constants, are defined in the Supplementary Material (Eq. (A4) for Scheme 1a) and detailed in Table 1, for the remaining mechanisms shown in Scheme 1. Bimolecular reactions are, therefore analytically described by a quotient of exponential functions with the same exponential argument and which are related to an hyperbolic

Table 1

Model dependent expressions of the primary constants and observed rate constant in Eqs. (1)–(5)

Mechanism	$\alpha$	$\beta$	$\gamma^a$	$\eta^b$
$\text{A} + \text{B} \rightleftharpoons \text{C} + \text{D}$	$k_1 - k_2$	$k_1(A_0 + B_0) + k_2(C_0 + D_0)$	$k_1A_0B_0 - k_2C_0D_0$	$\sqrt{k_1^2(A_0 - B_0)^2 + 4k_1k_2A_0B_0}$
$\text{A} + \text{B} \rightarrow \text{C} + \text{D}$	$k_1$	$k_1(A_0 + B_0)$	$k_1A_0B_0$	$k_1 A_0 - B_0 ^c$
$\text{A} + \text{B} \rightleftharpoons \text{C}$	$k_1$	$k_1(A_0 + B_0) + k_2$	$k_1A_0B_0 - k_2C_0$	$\sqrt{k_1^2(A_0 - B_0)^2 + k_2^2 + 2k_1k_2(A_0 + B_0)}$

The units of the primary constants are  $\alpha$ :  $\text{M}^{-1} \text{s}^{-1}$ ,  $\beta$ :  $\text{s}^{-1}$ ,  $\gamma$ :  $\text{M s}^{-1}$  and  $\eta$ :  $\text{s}^{-1}$ .

<sup>a</sup>  $\gamma$  is the initial velocity and is determined from the initial slope of Eq. (1) or (5). The corresponding analytical expressions are  $v_0 = x_{\text{EQ}}\eta/(1+\omega)$  and  $v_0 = \Delta A_{\text{EQ}}\eta/(1+\omega)$  (Eq. (A6) in the Supplementary Material), respectively, all terms being determined from the fits to the experimental data.

<sup>b</sup>  $\eta$  represents the observed rate constant or Eq. (2). With the exception of the irreversible mechanism, the reported expressions refer to the condition whereby initially only the reagents are present, which is usually the most simple experimental situation.

<sup>c</sup> The vertical bars indicate the absolute value.

tangent function (see Supplementary Material). When PFO conditions are met (i.e. when the initial concentrations of reagents are such that  $B_0 \gg A_0$ ), Eq. (1) reduces to the following expression:

$$x = A_0(1 - e^{-k_1 B_0 t})$$

Thus, under true pseudo-first order conditions the time course may be described by a simple exponential decay process with an apparent observed rate approaching  $k_1 B_0$ .

Eq. (1) breaks down to known equations as is in the case of irreversible bimolecular kinetics (Scheme 1b). Under these conditions the reverse reaction does not take place (i.e.  $k_2=0$ ) and Eq. (1) becomes (the vertical bars indicating the absolute value):

$$x = \frac{A_0 B_0 (1 - e^{-k_1 |A_0 - B_0| t})}{A_0 - B_0 e^{-k_1 |A_0 - B_0| t}}$$

which may be rearranged to the classically known equation used to graphically estimate bimolecular rate constants for irreversible reactions under PFO conditions (with  $B_0 > A_0$ , see Atkins [4]):

$$\frac{1}{A_0 - B_0} \ln \left\{ \frac{B_0(A_0 - x)}{A_0(B_0 - x)} \right\} = k_1 t$$

Eq. (1) also accounts for the case of binding kinetics (Scheme 1c). In this mechanism a compound binds reversibly to another to form a complex. In biochemistry this is specially the case of dioxygen-binding proteins such as myoglobins, hemoglobins (see the so-called Bible [5]) and in every enzyme encounter with substrate. In this case Eqs. (1)–(4) still hold, but the values of the  $\alpha$ ,  $\beta$ , and  $\gamma$  primary constants change as shown in Table 1.

**Experimental tests of Eqs. (1) and (2).** In order to test these equations I have carried out three stopped-flow experiments under non-PFO conditions, i.e. whereby the initial concentration of reagents is comparable in magnitude: (1) the ET reaction between ascorbate and hexacyanoferrate-III, an irreversible bimolecular reaction; (2) the ET reaction between the cytochrome *c* oxidase  $\text{Cu}_A$  and cytochrome  $c_{552}$  soluble domains from *P. denitrificans*, an example of a reversible reaction involving two substrates and two products with no experimentally demonstrated complex formed along the reaction coordinate and (3) carbon monoxide binding reaction to horse heart ferromyoglobin.

Fig. 1A shows the time course of reduction of hexacyanoferrate-III (ferricyanide) by ascorbate at pH 7 as determined by stopped-flow spectroscopy. In this reaction ascorbate passes an electron to ferricyanide (the redox potential difference is about 300 mV at pH 7, [6]), as followed by the decrease in absorbance at 420 nm and irreversibly generating the ascorbate radical and ferrocyanide. The time course was fitted to a simple exponential decay, a sum of 2 or more exponential processes and to a

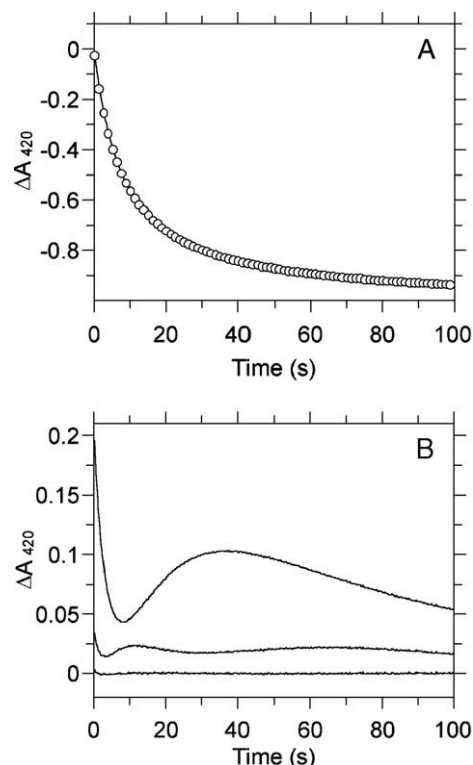


Fig. 1. (A) Time course of ferricyanide reduction by ascorbate as followed at 420 nm. A solution of 2.2 mM ferricyanide in 5 mM phosphate buffer pH 7.0 ( $T=293$  K) was mixed in the stopped-flow apparatus with a solution containing 1.2 mM ascorbate dissolved in the same buffer. Of the 400 experimental data points 80 are displayed for clarity (open circles). The solid line shows the best fit to Eq. (5) (readily derived from Eq. (1), see text and Supporting Information) with the following parameter values:  $\Delta A_{\text{EQ}} = -0.9966 \pm 0.0006$ ,  $\eta = 0.0052 \pm 0.0002 \text{ s}^{-1}$  and  $\omega = -0.958 \pm 0.001$ . The corresponding fits to a simple ( $y = a_1 \exp(-kt) + a_2$ ) or double ( $y = a_1 \exp(-k_{\text{FAST}}t) + a_2 \exp(-k_{\text{SLOW}}t) + a_3$ ) exponential process yield the following results:  $a_1 = 0.784 \pm 0.005$ ,  $k = 0.070 \pm 0.001 \text{ s}^{-1}$ ,  $a_2 = -0.914 \pm 0.001$  and  $a_1 = 0.499 \pm 0.003$ ,  $k_{\text{FAST}} = 0.182 \pm 0.001 \text{ s}^{-1}$ ,  $a_2 = 0.434 \pm 0.003$ ,  $k_{\text{SLOW}} = 0.0358 \pm 0.0003 \text{ s}^{-1}$ ,  $a_3 = -0.9481 \pm 0.0005$ , respectively. The solid line also shows the results obtained by numerical integration of the mechanism. (B) Plot of the residuals. The traces represent the differences between the experimental data and Eq. (5) (bottom), or the biexponential (middle) or monoexponential model (top). The bi- and monoexponential residuals are offset by 0.02 and 0.08 absorbance units for clarity.

modified form of Eq. (1) which takes into account the Lambert–Beer law (see Supplementary Material) since absorbance changes ( $\Delta A_\lambda$ ) are usually measured in stopped-flow experiments:

$$\Delta A_\lambda = \Delta A_{\text{EQ}} \frac{1 - e^{-\eta t}}{1 + \omega e^{-\eta t}} \quad (5)$$

Fig. 1B depicts a plot of the residuals, i.e. the difference between the experimental data and the specific fitting model. Clearly the simple exponential model is inadequate to account for the data, whereas the biexponential fit approximates much better the data although a non-random trend in the residuals is still present.

Fitting to sums of 3 or more exponential functions increased the quality of the fit considerably (not shown), but also yielded too many parameters (apparent rate constants

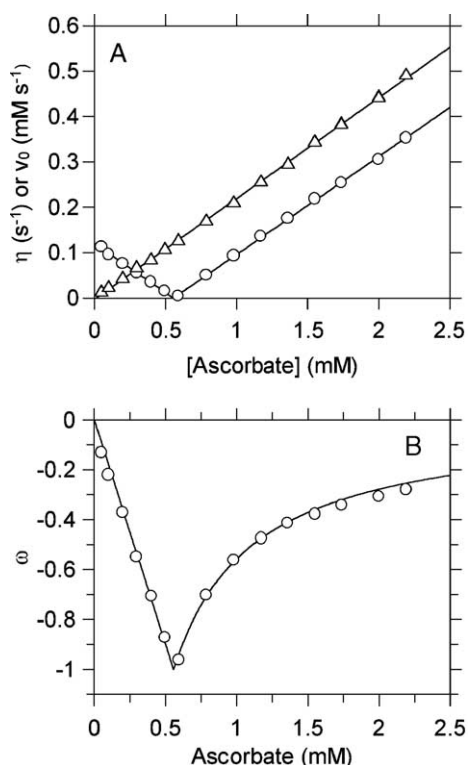


Fig. 2. Plot of the observed rate constants in the ascorbate–ferricyanide ET reaction. In this experiment the ascorbate concentration was systematically varied from 0.05 to 2.2 mM (after mixing) and the rate constant of reduction of ferricyanide determined by fitting the time courses to Eq. (5) (circles). The solid line is the best fit to Eq. (2) which is detailed in Table 1 and in the text. The triangles show the corresponding dependence of the initial velocities which are functions of the parameters in Eq. (5). Initial velocities are calculated by evaluation of the derivative of Eq. (5) with respect to time and extrapolation to time=0, i.e. the initial slopes of the time courses. The corresponding expression is given in the Supplementary Material, Eq. (A6). The solid lines also show the results obtained by numerical integration of the mechanism. Other conditions as in Fig. 1.

and amplitudes) with lack of significance in the physical interpretation of the data. This is due to the fact that the experiment was carried out under non-PFO conditions with comparable ascorbate and ferricyanide concentrations (see legends to Fig. 1). Eq. (5) which is readily derived from Eq. (1), on the other hand, yielded very good fits, as shown in Fig. 1, since it was derived in a most general way with no bias on the relative concentrations of the reagents. When the ascorbate initial concentration was systematically varied while keeping ferricyanide concentration constant, similar time courses to that shown in Fig. 1A were obtained. The data were fitted to Eq. (5) and the observed rate constants ( $\eta$ , i.e. Eq. (2)) are plotted against the initial ascorbate concentration in Fig. 2A.

The most striking result of this experiment is that as ascorbate concentration is changed, the observed rate constant linearly decreases (from 0.11 to 0.016 s<sup>-1</sup>, as ascorbate concentration is increased from 0.05 to 0.49 mM, see Fig. 2A, open circles) and after reaching a minimum very close to zero steadily increases linearly. The slopes of

the descending and ascending parts of the graph may be shown to represent the apparent second-order rate constant and (the absolute values) are identical within the experimental error ( $213 \pm 6$  and  $214 \pm 2$  M<sup>-1</sup> s<sup>-1</sup>, respectively). Fig. 2A also shows that initial velocities, as determined from the initial slopes of the time courses (see Supplementary Material, Eq. (A6)), nevertheless increase in the entire concentration range (open triangles) as expected since in any bimolecular reaction the initial rates are linear functions of the reagent and product concentrations.

The decrease in the observed rate constant is predicted by Eq. (2). By substituting the appropriate values of the primary constants in the expression of  $\eta$  (see Table 1), it follows that the observed rate constant is proportional to the difference in the initial concentrations of the reagents. This behaviour is due to setting the experimental conditions to mostly non-PFO. As discussed above, the time-dependent changes may deviate substantially from a simple exponential decay process. This is critically determined by the relative concentrations of the reagents and specifically by the value of the  $\omega$  parameter in Eqs. (1) and (5) which is defined in Eq. (4). Fig. 2B shows for this very experiment the dependence of  $\omega$  on the initial ascorbate concentration as determined by the fits to the experimental data. In the case of an irreversible reaction (Scheme 1b),  $\omega$  has values in the  $-1 < \omega < 0$  range. The closer the value of this parameter to zero, the more exponential the time course will appear, this being the case at low or high ascorbate concentrations relative to the initial ferricyanide concentration. As seen in Fig. 2B,  $\omega$  decreases from zero at low ascorbate concentration and thereafter increases after passing through  $-1$ , a situation whereby the reagents approach the most stringent bimolecular condition for the mechanism depicted in Scheme 1b. As numerical simulations predict (not shown) the  $\omega$  parameter achieves different values depending on the specific mechanism. These results are shown in Table 2.

In the second experiment the ET reaction between cytochrome *c* oxidase Cu<sub>A</sub> and cytochrome *c*<sub>552</sub> soluble domains from *P. denitrificans* was studied. These two engineered proteins are very good models for the initial ET processes between cytochrome *c* oxidase and cytochrome *c* without the ensuing complications due to the subsequent ET events between the Cu<sub>A</sub> site in subunit II and cytochrome *a* in subunit I, the latter dominating the absorption spectrum. Moreover, recent NMR chemical shift perturbation mapping experiments [7] suggest that this ET couple does not form a stable complex to any significant extent. The reaction was studied both in forward direction (mimicking the physio-

Table 2  
Model dependent values of the  $\omega$  parameter (Eq. (4))

Mechanism	$\omega$		
A+B=C+D	$k_1 > k_2$	$k_1 = k_2$	$k_1 < k_2$
	$-1 < \omega < 0$	0	$0 < \omega < 1$
A+B→C+D	$-1 < \omega < 0$		
A+B=C	$-1 < \omega < 0$		



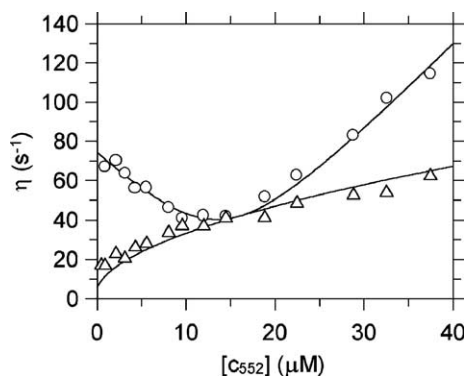


Fig. 3. Electron transfer reaction between the  $\text{Cu}_A$  and cytochrome  $c_{552}$  soluble domains from *Paracoccus denitrificans*. Oxidized or reduced 30  $\mu\text{M}$   $\text{Cu}_A$  domain was mixed against varying concentrations of ferro- or ferricytochrome  $c_{552}$  (ca. 1 to 80  $\mu\text{M}$ ). Pre-reduction of either protein was achieved by adding 0.5 mM ascorbate to the chosen protein solution as described previously [2]. The time courses were fit to Eq. (5) and the determined rate constants are plotted as a function of ferrocytochrome  $c_{552}$  (forward direction, triangles) or ferricytochrome  $c_{552}$  (reverse direction, circles). Solid lines represent the simultaneous fit of both data sets to Eq. (2) with parameters given in the text and also the results obtained by numerical integration of the mechanism.

logical situation) in which ferrocytochrome  $c_{552}$  donates an electron to the oxidized  $\text{Cu}_A$  domain, and in the reverse direction according to a protocol which uses ascorbate [2]. When the observed rate constants for these processes (obtained from the fits of the time courses to Eq. (5)) are plotted as a function of (ferro- or ferri-) cytochrome  $c_{552}$ , Fig. 3 is obtained, the solid lines resulting from the simultaneous fit of the complete data set to Eq. (2).

The determined values of the forward and reverse rate constants ( $k_1$  and  $k_2$  in Scheme 1a) are  $3.8 \cdot 10^5 \pm 2 \cdot 10^4$  and  $4.6 \cdot 10^6 \pm 10^5 \text{ M}^{-1} \text{ s}^{-1}$  and in very good agreement with a preceding study ( $8.3 \cdot 10^5$  and  $5.0 \cdot 10^6 \text{ M}^{-1} \text{ s}^{-1}$  respectively, see Maneg et al. [2]) at the same ionic strength and

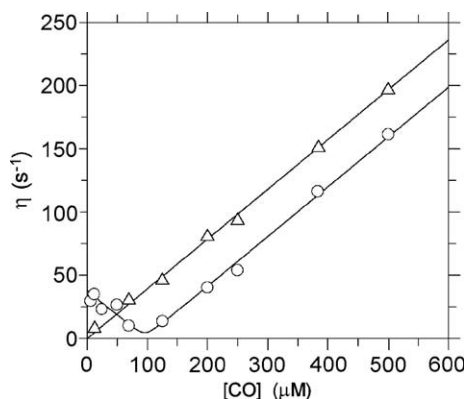


Fig. 4. CO binding to ferrous myoglobin. The plot shows the CO concentration dependence of the observed rate constants determined by fitting the experimental time courses to equation [5]. The myoglobin concentration was 100 (circles) or 1  $\mu\text{M}$  (triangles) after mixing. Solid lines represent the best fit to Eq. (2) (see Table 1) with parameters given in the text.

temperature. The shapes of the curvilinear plots are deeply different in the two directions with an upward (with  $-1 < \omega < 0$ ) and downward (with  $0 < \omega < 1$ ) concavity in the reverse (Fig. 3, open circles) and forward (Fig. 3, open triangles) reaction, respectively, features which are predicted by Eq. (2) (see also Tables 1 and 2). From a qualitative point of view, a bimolecular reaction studied in the direction to the right in Scheme 1a that yields an  $\eta$ -vs.-reagent concentration plot with a downward concavity will immediately indicate that  $k_1 < k_2$  and therefore thermodynamic information. In the reverse reaction (Fig. 3, open circles), a decrease in  $\eta$  is also observed at low ferricytochrome  $c_{552}$  concentrations as in the ascorbate–ferricyanide reaction (Fig. 2A).

In the third experiment ferrous horse heart myoglobin was mixed with a solution containing varying concentrations of CO (from ca. 6 to 500  $\mu\text{M}$ , after mixing). In this reaction myoglobin reversibly binds carbon monoxide to yield the carbonylated adduct. CO binding was studied out at two myoglobin concentrations, 1 and 100  $\mu\text{M}$  (after mixing) which determine PFO and non-PFO conditions and exponential or multiexponential time courses, respectively. In both cases the time courses were fit to Eq. (5) and the observed rate constants are plotted in Fig. 4. The plots are dramatically different depending on the initial myoglobin concentration and under non-PFO conditions at low CO concentrations  $\eta$  decreases as predicted by Eq. (2). The determined rate constants are  $3.9 \cdot 10^5 \pm 10^4 \text{ M}^{-1} \text{ s}^{-1}$  and  $0.2 \pm 0.7 \text{ s}^{-1}$  in excellent agreement with literature values [5].

#### 4. Final comments

In this investigation I have demonstrated by theory and experiment that the time evolution of bimolecular reactions is accounted for by a quotient of exponential functions. A general expression, independent of the experimental setup, has been derived (Eqs. (1) and (5)) which accurately describes the time course of second-order processes of several types (see Scheme 1). The observed rate constant ( $\eta$  in Eq. (2)) shows a complex dependence on the initial reagent concentration being varied  $B_0$ , yet instantaneously indicates the ergonicity of the reaction, since exoergonic reactions will appear with an upward concavity and a negative  $\omega$  value in the  $\eta$ -vs.- $B_0$  plot, whereas in endoergonic reactions the opposite is true (with  $0 < \omega < 1$ ). Second-order reactions may of course be studied under PFO conditions which yield simple exponential time courses and linear PFO plots. However, in several experimental situations these conditions are difficult to achieve: (i) when the half-time of the reaction is comparable to the dead-time of the instrument (i.e. normally a stopped-flow apparatus); (ii) when spectral overlap of reagents and/or products with high extinction coefficients saturates the response of the photomultiplier tube; (iii) when the availability of materials is

limiting, which is often the case of genetically engineered proteins which are loosely expressed; and (iv) when the second-order reaction takes place between reaction intermediates, as may be the case of protein folding [8]. Furthermore the expectations of Eq. (1) indicate that in self-exchange electron transfer reactions [9] (Scheme 1a with  $k_1=k_2$ ), the time course will appear monoexponential at any reagent/product concentration.

### Acknowledgements

This paper is dedicated to my Professor, Maurizio Brunori, an outstanding scientist, teacher and friend. I thank Oliver Maneg and Bernd Ludwig (Frankfurt University) for providing the Cu<sub>A</sub> and cytochrome *c*<sub>552</sub> soluble domain samples for the experiment in Fig. 3. I also wish to thank Richard W. Hendler and Richard I. Schragar (NIH, Bethesda) for comments and criticism at initial stages of this work, Gino Amiconi, Stefano Gianni and Carlo Travaglini-Allocatelli (University of Rome “La Sapienza”) and Massimiliano Aschi (University of L’Aquila) for their interest. Work was partially supported by a Programma di Ricerca Scientifica Interuniversitario Nazionale (PRIN 2003) entitled “Bioenergetica: genomica funzionale, meccanismi molecolari ed aspetti fisiopatologici”.

### Appendix A. Supplementary data

Supplementary data associated with this article can be found, in the online version, at [doi:10.1016/j.bpc.2005.04.006](https://doi.org/10.1016/j.bpc.2005.04.006).

### References

- [1] B. Reincke, L. Thony-Meyer, C. Dannehl, A. Odenwald, M. Aidim, H. Witt, H. Ruterjans, B. Ludwig, *Biochim. Biophys. Acta* 1411 (1999) 114–120.
- [2] O. Maneg, B. Ludwig, F. Malatesta, *J. Biol. Chem.* 278 (2003) 46734–46740.
- [3] K.J. Laidler, *Chemical Kinetics*, Harper and Row, New York, 1987.
- [4] P.W. Atkins, *Physical Chemistry*, IV edition, Oxford University Press, Oxford, UK, 1990.
- [5] E. Antonini, M. Brunori, *Hemoglobin and Myoglobin in their Reactions with Ligands*, North Holland Publishing Company, Amsterdam, 1971.
- [6] G.D. Fasman (Ed.), *CRC Handbook of Biochemistry and Molecular Biology*, 3rd ed., Physical Chemical Data, vol. I, CRC Press, Cleveland, OH, 1976, pp. 122–130.
- [7] H. Wienk, O. Maneg, C. Lücke, P. Pristovšek, F. Løhr, B. Ludwig, H. Rüterjans, *Biochemistry* 42 (2003) 6005–6012.
- [8] D.E. Otzen, O. Kristensen, M. Oliveberg, *Proc. Natl. Acad. Sci. U. S. A.* 97 (2000) 9907–9912.
- [9] R.A. Marcus, N. Sutin, *Biochim. Biophys. Acta* 811 (1985) 265–322.